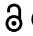



ORIGINAL RESEARCH

 OPEN ACCESS 

## A novel Fc-enhanced humanized monoclonal antibody targeting B7-H3 suppresses the growth of ESCC

Huiting Wu<sup>a,b\*</sup>, Chang Liu<sup>a,b\*</sup>, Qiang Yuan<sup>a,b\*</sup>, Yan Qiao<sup>a,b</sup>, Yongwei Ding<sup>c</sup>, Lina Duan<sup>a,b</sup>, Wenjing Li<sup>a,b</sup>, Mengjia Zhang<sup>a,b</sup>, Xuhua Zhang<sup>d</sup>, Yanan Jiang<sup>a,b</sup>, Jing Lu<sup>a,b</sup>, Ziming Dong<sup>a,b</sup>, Tao Wang<sup>e,f</sup>, Kangdong Liu<sup>a,b,g</sup>, and Jimin Zhao<sup>a,b,g</sup>

<sup>a</sup>Department of Pathophysiology, School of Basic Medical Sciences, Zhengzhou University, Zhengzhou, China; <sup>b</sup>Henan Provincial Cooperative Innovation Center for Cancer Chemo- prevention, Zhengzhou, China; <sup>c</sup>Department of Pathophysiology, Shaoxing People Hospital, Shaoxing, China; <sup>d</sup>The Affiliated Cancer Hospital, Zhengzhou University, Zhengzhou, China; <sup>e</sup>Telethon Kids Institute, University of Western Australia, Perth, Australia; <sup>f</sup>The College of Nursing and Health, Zhengzhou University, Zhengzhou, China; <sup>g</sup>State Key Laboratory of Esophageal Cancer Prevention and Treatment, Zhengzhou University, Zhengzhou, China

### ABSTRACT

Esophageal squamous cell carcinoma (ESCC) is a prevalent malignant tumor of the digestive tract with a low 5-year survival rate due to the lack of effective treatment methods. Although therapeutic monoclonal antibodies (mAbs) now play an important role in cancer therapy, effective targeted mAbs are still lacking for ESCC. B7-H3 is highly expressed in a variety of tumors and has emerged as a promising therapeutic target. Several mAbs against B7-H3 have advanced to clinical trials, but their development has not yet been pursued for ESCC. Here, we developed a humanized and Fc-engineered anti-B7H3 mAb 24F-Hu-mut2 and systematically evaluated its anti-tumor activity *in vitro* and *in vivo*. The 24F-Hu-mut2 was humanized and modified in Fc fragment to obtain stronger antibody-dependent cell-mediated cytotoxicity (ADCC) activity and nanomolar affinity. Furthermore, both of ESCC cell-derived xenograft (CDX) and patient-derived xenograft (PDX) mice models indicated that 24F-Hu-mut2 displayed potent *in vivo* anti-tumor activity. In addition, a computational docking model showed that the mAb bound to IgC1 and IgC2 domain of B7-H3, which is closer to the cell membrane. Consistently, our ELISA results verified the binding of 24F-Hu-WT and IgC1 and IgC2. Our results indicate that 24F-Hu-mut2 has significant anti-ESCC activity both *in vitro* and *in vivo*, and this monoclonal antibody may be a promising antibody against ESCC and other B7-H3 overexpressing tumors.

### ARTICLE HISTORY

Received 20 April 2023  
Revised 6 November 2023  
Accepted 7 November 2023

### KEYWORDS

ADCC; B7-H3; Esophageal squamous cell carcinoma; Fc engineering; monoclonal antibody

## Introduction


Esophageal Squamous cell carcinoma (ESCC) is the predominant type of esophageal cancer, which is prevalent in South Africa, Central Asia, and China.<sup>1</sup> Due to the limited therapeutic efficacy of surgery, radiotherapy, and chemotherapy, the overall 5-year survival rate of ESCC patients is less than 20%.<sup>2</sup> Therefore, there is an urgent need for new effective treatment for ESCC. Immunotherapy has emerged as an important pillar in the field of cancer therapy in recent decades. Therapeutic monoclonal antibody (mAb) is one of the main means of immunotherapy, which has the advantages of high targeting, strong specificity, mild side effects and so on. It has been used in the clinical treatment of some malignant tumors. Monoclonal antibody drugs can act through a variety of mechanisms after entering the body. On one hand, The antigen-binding fragment of an antibody recognizes the antigen and prevents antigen from binding to its ligand, thereby preventing tumor cell proliferation, migration, immune escape, etc. For instance, monoclonal antibodies targeting PD1 can activate the immune system to eliminate tumors by blocking the binding of PD1 to its ligands; On the other hand, tumor

cells can be eliminated by antibody-dependent cell-mediated cytotoxicity (ADCC), antibody-dependent cell-mediated phagocytosis (ADCP), complement-dependent cell-mediated cytotoxicity (CDC) and other functions. Among them, ADCC is an effective cytotoxic mechanism, mainly mediated by NK cells, which is the basis of the effect mechanism of a variety of antibody drugs such as rituximab, daratumumab, and trastuzumab. Enhancing ADCC effect is an important direction of antibody-drug engineering. It provides a new possibility for ESCC treatment.

B7-H3, a member of the B7 family, is abnormally expressed in a variety of malignancies, and is not expressed or low expressed in normal tissues.<sup>3,4</sup> Importantly, B7-H3 expression is closely related to the occurrence and development of tumors and poor prognosis.<sup>5,6</sup> Although the receptor of B7-H3 has not been fully identified, B7-H3 has been experimentally implicated in the transmission of costimulatory and inhibitory signals of the immune system.<sup>7</sup> As suggested by some recent investigations, B7-H3 has an inhibitory effect on the immune response, which facilitates tumor cells to evade immune surveillance.<sup>8,9</sup> In recent years, studies have shown that B7-H3 is highly expressed in ESCC and

**CONTACT** Jimin Zhao  [zhaojimin@zzu.edu.cn](mailto:zhaojimin@zzu.edu.cn); Kangdong Liu  [kdliu@zzu.edu.cn](mailto:kdliu@zzu.edu.cn)  Department of Pathophysiology, School of Basic Medical Sciences, Zhengzhou University, Zhengzhou, China

\*Huiting Wu, Chang Liu and Qiang Yuan are contributed equally to this study.

 Supplemental data for this article can be accessed online at <https://doi.org/10.1080/2162402X.2023.2282250>

© 2023 The Author(s). Published with license by Taylor & Francis Group, LLC.

This is an Open Access article distributed under the terms of the Creative Commons Attribution-NonCommercial License (<http://creativecommons.org/licenses/by-nc/4.0/>), which permits unrestricted non-commercial use, distribution, and reproduction in any medium, provided the original work is properly cited. The terms on which this article has been published allow the posting of the Accepted Manuscript in a repository by the author(s) or with their consent.

is associated with poor prognosis of ESCC.<sup>10</sup> These characteristics suggest that B7-H3 may become a new target for ESCC treatment. At present, several antibodies targeting B7-H3 have entered pre-clinical or clinical studies, among which mAbs MGA271 (MacroGenics) and 8H9 (Y-MAbs Therapeutics) have achieved significant efficacy in the treatment of non-small cell lung cancer, neuroblastoma and other solid tumors in clinical trials.<sup>11,12</sup> However, the role of anti-B7-H3 mAbs in the treatment of ESCC has been rarely studied, and its efficacy is unclear.

In this study, we develop a novel monoclonal antibody against B7-H3 for ESCC treatment. Firstly, we obtained the original anti-B7-H3 mAbs by immunizing mice with antigens and hybridoma screening. The antibody with the highest affinity was then humanized and named 24F-Hu-WT. Next, two forms of Fc engineering were utilized to enhance the efficiency of ADCC of 24F-Hu-WT, without compromising the original affinity as confirmed by Surface Plasmon Resonance (SPR). One of the Fc-engineered antibodies, 24F-Hu-mut2, exhibited significant anti-tumor activity against B7-H3-expressing ESCC cells *in vitro* and *in vivo*. To facilitate additional modification and engineering, we also explored the binding region of 24F-Hu-WT on B7-H3 protein, and found that it mainly bound to IgC1 and IgC2 domains of B7-H3. Our results suggest that the Fc-enhanced mAb 24F-Hu-mut2 may provide a potential therapeutic agent for ESCC therapy.

## Materials and methods

### Cell lines

Human ESCC lines KYSE30, KYSE150, KYSE410, KYSE450, KYSE510, TE-1, and human embryonic kidney cell HEK293F were preserved and provided by the Department of Pathophysiology, Basic Medical College of Zhengzhou University. Human ESCC cell lines KYSE30, KYSE150, KYSE410, KYSE450 and TE-1 were cultured in RPMI 1640 medium containing 10% FBS. KYSE510 cells were cultured in DMEM medium containing 10% FBS. HEK293F cells were cultured in serum-free medium 293T-II (Sino Biological Inc., China). All cells were grown in a humidified incubator containing 5% CO<sub>2</sub> at 37°C.

### Immunohistochemistry (IHC)

Tissue microarrays from Henan Cancer Hospital were deparaffinized and hydrated. Antigen retrieval was completed by immersing slides in citric acid retrieval solution under pressure for 10 min. Then, the slides were treated with 3% H<sub>2</sub>O<sub>2</sub> for 10 min at room temperature, followed by overnight incubation at 4°C with primary antibodies against B7-H3 (Cell Signaling Technology, Catalog No.14058T). The next day, the slides were developed using a two steps detection kit (ZSGB-BIO, Catalog SAP-9100) and DAB chromogen, and counterstained with hematoxylin. The slides were quantified by calculating the percentage of positive cells using the Image-Pro Plus software (v.6.0).

### Generation of monoclonal antibody

Female Balb/c mice (Henan Laboratory Animal Center) were immunized with B7-H3-4Ig protein (Acro Biosystems. Catalog No.B7B-H52E7). The protein was mixed with adjuvant and

injected subcutaneously into mice once a fortnight. After the third immunization, the serum titer of the mice was measured, and the one with the highest titer was selected for shock immunization. The mouse spleen cells were fused with myeloma cells to form hybridoma cells. Anti-B7-H3 hybridoma supernatant was tested by ELISA. Monoclonal hybridoma cells that produced the monoclonal antibody were sequenced to identify the sequence-specific mAb.

### Expression of antibodies

The light and heavy chain plasmids of the antibody (2 µg/mL) and PEI (1 mg/mL, Polysciences. Catalog No. 23966-1) were added to the medium, mixed, and incubated for 5 min at room temperature, respectively. The PEI-containing medium was then transferred to the plasmid-containing medium, and incubated together for 20 min. The ratio of plasmid to PEI was 1:3. The density of HEK293F cells was adjusted to 4 × 10<sup>6</sup>/mL. The mixed medium was added to the cell suspension and placed at 37°C in a 5% CO<sub>2</sub> incubator with a shaker. On the second day of transfection, the temperature of the incubator was cooled to 32°C, and a supplement (Sino biological. Catalog No. M293-SUPI) and glutamine were added to the culture system every 48 h. The cell viability was continuously recorded, and if the cell viability was lower than 70%, the protein expression procedure was terminated. The cell suspension was transferred to a centrifuge tube at 800 g for 10 min. The supernatant was collected.

### Antibody purification

The antibody was purified using a Hitrap 1 mL Mabselect SuRe (Cytiva. Catalog No. 11003493) purification column at a flow rate of 1 mL/min. After sample loading, the PBS buffer was replaced, the flow rate was set at 1 mL/min, and the column was rinsed until equilibrium. The eluate was replaced with 100 mM glycine eluate (pH 2.7) at a flow rate of 1 mL/min. The pH of the eluate was adjusted to neutral using pH 8.0 Tris-HCl. The antibody was transferred to a dialysis bag with a 14 KD cutoff molecular weight for dialysis, collected, and the antibody concentration was measured by using Nanodrop one (Thermo Scientific).

### Antibody humanization

Amino acid sequences of variable light chain (VL) and variable heavy chain (VH) were designed using the complementary determining region (CDR) sequences from the mouse 24F7H mAb and framework sequences from human germline V-kappa or VH segment, respectively. The humanized VL and VH coding sequences were synthesized *de novo*, and fused to the human C-kappa or human gamma1 constant region cDNA, respectively.

### Fc engineering

We made two types of Fc engineering modifications of the heavy chain of 24F-Hu-WT antibody to enhance the effect of ADCC. 24F-Hu-mut5 was designed to mutate 5 amino acids (L235V, F243L, R292P, Y300L and P396L) in the Fc domain, which is the same as the Fc sequence of positive control MGA271<sup>12</sup> 24F-

Hu-mut2 mutated 2 amino acids (S239D, I332E), which was referenced the Fc engineering of anti-CD19 mAb XmAb5574.<sup>13</sup>

### Flow cytometry

Cells were digested in non-enzyme cell detach solution. Then cell samples were treated with primary antibody (2 µg/ml) for 1 h at 4°C, and stained with FITC-conjugated affinity-pure Goat-anti-Human IgG (Proteintech Catalog No. SA00003-12) at 4°C in the dark. Cells were analyzed using a flow cytometer (Agilent NovoCyte) and FlowJo software.

### ELISA

An ELISA plate was coated with soluble human B7-H3-4Ig or B7-H3-2Ig (2 µg/ml) in PBS overnight at 4°C. The plate was blocked with PBS containing 5% milk for 2 h at room temperature. Antibodies were diluted in PBS and applied to the ELISA plate for 2 h. Following washing with PBS containing 0.2% Tween 20 (PBST), HRP conjugated goat anti-mouse IgG or goat anti-human IgG were incubated for 1 h (dilution 1:5000 in PBS). The plate was washed and developed with 100 µL/well of TMB peroxidase substrate and terminated with 100 µL/well of 1 M HCl. Absorbance at 450 nm was determined and data analyzed using GraphPad Prism 8 software.

### Antibody-dependent cell-mediated cytotoxicity

Peripheral blood mononuclear cells (PBMCs) were isolated from the blood of healthy donors by density gradient centrifugation using lymphocyte isolation solution. Then, the PBMCs were induced by 200 U/mL of IL-2 for 24 h. Subsequently, ESCC cells were incubated with PBMCs at effector:target (E:T) ratios of 20:1 overnight, in which serially diluted antibodies were added. The lactate dehydrogenase (LDH) release was measured by CytoTox 96° NonRadioactive Cytotoxicity Assay kit (Promega Corp. Catalog No. G1780). The Cytotoxicity of antibodies was determined as: Cytotoxicity (%) = (experimental cell lysis - antibody-independent cell cytolysis) / (maximum target lysis - spontaneous target lysis) × 100%.

### Affinity measurements

The binding affinity of 24F-Hu-WT, 24F-Hu-mut2 or MGA271 against human B7-H3-4Ig protein (Acro Biosystems. Catalog No. B7B-H52E7) was analyzed by surface plasmon resonance using Biacore T200 (GE Healthcare). Monoclonal antibodies were immobilized to protein A chip, and then B7-H3 protein was injected. Binding curves were obtained. The KD values were calculated using Biacore T200 Evaluation Software (version 4.1.1).

### Computer docking model

The structure of the B7-H3 antigen was predicted by AlphaFold v2.0,<sup>14,15</sup> while the 24F-Hu-WT antibody was predicted by Rosetta antibody protocol.<sup>16-20</sup> Afterwards, the docking simulation was performed by using ZDOCK 3.0.2.<sup>21</sup> At last, the complexes were minimized by using AMBER16 program.

## Cell-Derived Xenograft (CDX) and Patient-Derived Xenograft (PDX) mouse models

All mouse experiments were carried out under protocols approved by the Ethics Committee of Zhengzhou University (ZZUIRB2023154). Female SCID mice (which have functional NK cells and macrophages) aged 4–6 weeks were purchased from Cyagen Biosciences and maintained in SPF grade animal laboratories. The mice were fed with special feed and drinking water after sterilization. KYSE150 cells ( $2.5 \times 10^6$  per mouse) in PBS and patient-derived ESCC tissues EG20 were subcutaneously implanted into mice, respectively. When tumors were approximately 50 to 100 mm<sup>3</sup>, antibodies were administered intraperitoneally once weekly for 3–4 weeks at a dosage of 5 mg/kg. Tumor sizes were monitored twice weekly by orthogonal measurements with electronic calipers.

### Statistical analysis

All quantitative results were expressed as mean values ± SD and  $P < .05$  were considered statistically significant. Significant differences were determined by Student's *t*-test or one-way ANOVA using GraphPad Prism 8.0 or SPSS 22.0 software.

## Results

### B7-H3 is highly expressed in human ESCC tissues and cell lines

The Cancer Genome Atlas (TCGA) database suggested the protein levels of B7-H3 were up-regulated on multiple tumors including ESCC, compared to the corresponding para-carcinoma tissue (Figure 1a). Moreover, the expression level of B7-H3 transcripts was increased compared with normal tissues in different types and stages of esophageal cancer, (Figure 1b,c). To further validate B7-H3 expression in ESCC, we examined the protein levels of B7-H3 in an ESCC tissue array by immunohistochemistry. The results showed that the protein levels of B7-H3 were higher in ESCC tissues ( $n = 63$ ) compared to adjacent tissues ( $n = 27$ ), and the difference was statistically significant ( $p < .001$ ). Representative case images and statistical results of the tumor and adjacent tissues were shown in Figure 1d-e. In addition, we detected the protein levels of B7-H3 in ESCC cell lines by flow cytometry with a positive antibody MGA271 as the primary antibody. The results showed that B7-H3 expression was higher in ESCC cell lines (Figure 1f). These results indicate that B7-H3 protein levels are up-regulated in ESCC compared to para-carcinoma tissue.

### 24F7H shows strong binding activity to B7H3 and ESCC cells

BALB/C mice were immunized with B7-H3-4Ig protein mixed with adjuvant. For the first immunization, complete adjuvant and protein were mixed into an emulsified state and injected subcutaneously into mice at split-point. The second and third immunizations used incomplete adjuvants mixed with protein. The interval between the two immunizations was 2 weeks. After three immunizations, serum titers of mice were measured

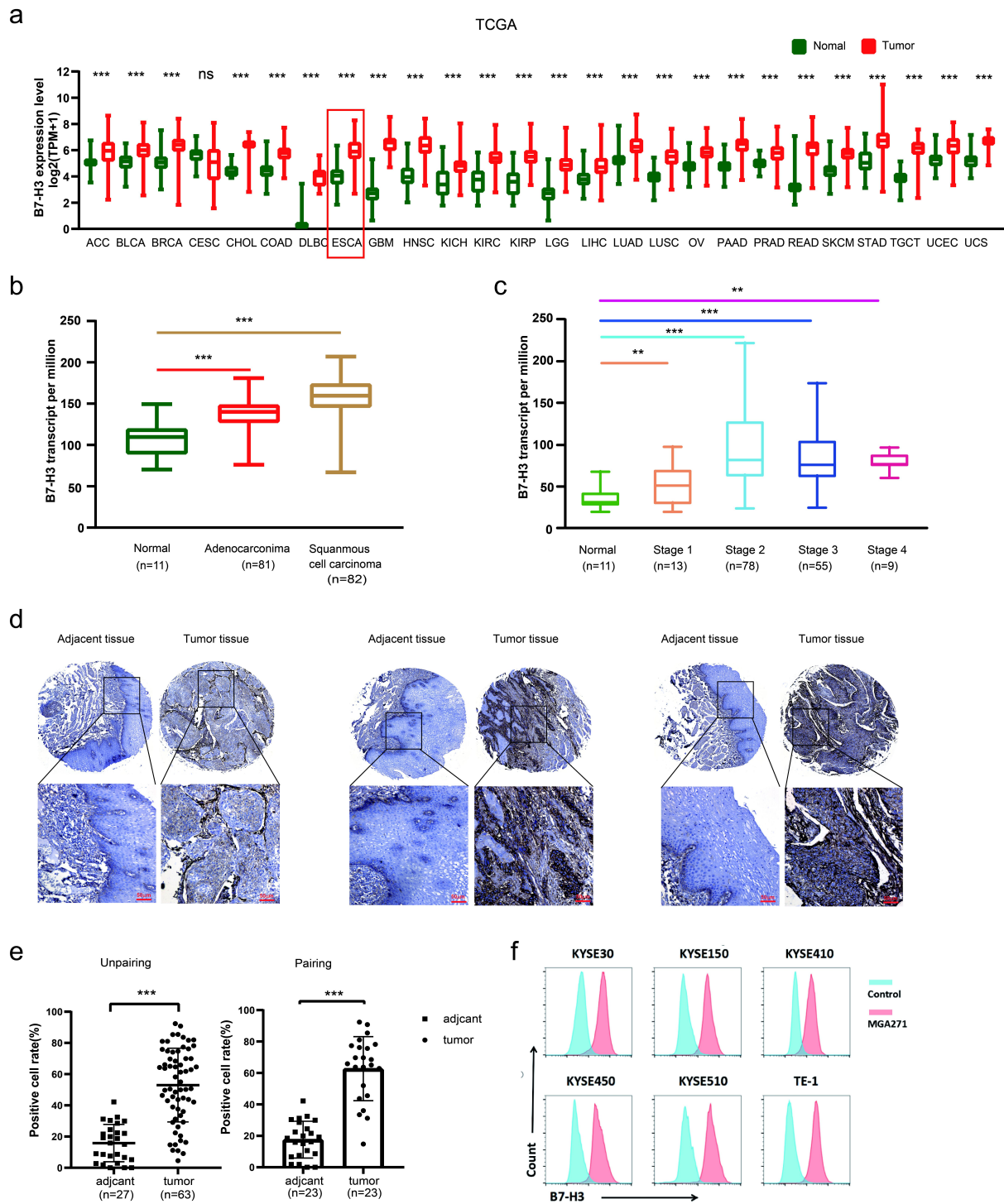


**Figure 1.** B7H3 is highly expressed in ESCC tissues and cell lines. (a) Differential expression profile analysis of B7-H3 in tumor and adjacent tissues based on the TCGA database. (b) The transcript expression levels of B7-H3 in different types of esophageal cancer tissues were analyzed based on TCGA database. (c) The transcript expression levels of B7-H3 in different stages of esophageal cancer were analyzed based on TCGA database. (d) Representative images of immunohistochemistry staining of B7-H3 in ESCC tissue microarrays were shown. (e) Statistical graph of the tissue microarray unpairing and pairing analysis. (f) Flow cytometry results of B7-H3 expression in ESCC cells and MGA271 is a positive antibody to B7-H3. All data are shown as means $\pm$ S.D. The asterisks (\*, \*\*, \*\*\*) indicate statistical significance ( $p < .05$ ,  $p < .01$ ,  $p < .001$ , respectively).

by ELISA. The one with the highest titer was selected for shock immunization. After four immunizations, mouse spleen cells were fused with myeloma cells to obtain hybridoma cells capable of producing antibodies. The supernatant of hybridoma pools binding to both of B7H3-4Ig and B7H3-2Ig proteins was screened by ELISA. Subsequently, four murine mAbs were

obtained, named 7F5A6, 7F5B10, 19D8G and 24F7H, respectively. The binding ability of these four mAbs to ESCC KYSE150 and KYSE450 cells was determined by flow cytometry, with MGA271 serving as a positive control. The results showed that the binding ability of the four mAbs to KYSE450 cells was higher than MGA271 (Figure 2a). To further validate

the binding ability of the four mAbs to the B7-H3 protein and cells. B7-H3 proteins were diluted to a series of concentrations, and the EC50 values of mAbs bound to the protein and cells were determined by ELISA and flow cytometry. The results indicated that the EC50 values of 24F7H binding to B7-H3-2Ig, B7-H3-4Ig and KYSE150 cells were  $49.1 \pm 2.3$  ng/ml,  $33.1 \pm 0.04$  ng/ml and  $508.7 \pm 63.2$  ng/ml, respectively. Compared with other antibodies, the binding affinity of 24F7H to B7-H3 was the highest (Figure 2b-c and Supplement Table S2), which possesses the potential for further modification. Given the immunogenicity of the murine monoclonal antibody to human, we humanized the murine antibody of 24F7H, to facilitate its clinical application. The complementary determining regions (CDR) of 24F7H were grafted onto the human immunoglobulin G (IgG) frameworks, named 24F-Hu-WT.

### The Fc-engineered antibody 24F-Hu-mut2 shows high affinity to B7-H3 protein and anti-tumor activity in vitro

Subsequently, we used liquid chromatography to check antibody purity. The purity of 24F-Hu-mut2, 24F-Hu-WT and 24F-Hu-mut5 was 88.98%, 88.07% and 91.40%, respectively (Supplement Figure S1B and Supplement Table S1). The purified protein was confirmed by the results of reductive SDS-PAGE and non-reductive SDS-PAGE. The molecular weight of the antibody was about 150KD and no obvious miscellaneous bands were observed (Supplement Figure S1A). In order to enhance the activity of antibody-mediated ADCC, we modified the Fc region of the mAb 24F-Hu-WT in two forms to enhance the affinity of Fc to the FcRIIIa. One mutant, 24F-Hu-mut5, was generated from 24F-Hu-WT by exchanging 5 amino acids (aa) of the Fc domain (i.e., L235V, F243L, R292P, Y300L and P396L, same as MGA271), and the other mutant, 24F-Hu-

mut2, was generated by exchanging 2 aa residues same as anti-CD19 mAb XmAb5574 (i.e., S239D, I332E). In order to confirm whether the Fc-optimization affects the binding of the antibody to its antigen, B7-H3 was diluted into various concentrations, and the EC50 value of binding between monoclonal antibodies and B7-H3 protein was detected by ELISA. Simultaneously, the binding capacity of 24F-Hu-WT, 24F-Hu-mut2, 24F-Hu-mut5 to KYSE150 cells was also assessed by flow cytometry. ELISA and flow cytometry results showed that the EC50 value of the modified antibody did not change significantly Figure 3a,b and (Supplement Table S3).

To evaluate the effect of amino acid mutation in the Fc region of mAbs on its binding to B7-H3, the KD values of 24F-Hu-WT, 24F-Hu-mut2 and 24F-Hu-mut5 were assessed by SPR (Figure 3c-f). The affinity of 24F-Hu-mut2, 24F-Hu-mut5 and 24F-Hu-WT to human B7-H3-4Ig was 0.5 nM, 0.53 nM and 0.8 nM, respectively, whereas the KD value of the positive control MGA271 was 1.43 nM (Table 1). The results showed that the affinity of 24F-Hu-mut2 and 24F-Hu-mut5 did not decrease significantly compared with 24F-Hu-WT, and the affinity of the modified 24F7H mAb was higher than that of the positive control MGA271. Next, to investigate whether the ADCC activity of Fc-optimized antibodies was enhanced, we conducted the LDH assay. The results showed that 24F-Hu-mut2 maintained a strong inhibitory effect on tumor cells. The ADCC activity of 24F-Hu-mut2 was higher than that of 24F-Hu-WT, 24F-Hu-mut5 and MGA271 (Figure 3g-j). Compared to 24F-Hu-WT, the tumor inhibitory rate of 24F-Hu-mut2 increased by 10%-15%. In addition, the PBMC cells of mice were separated and incubated with ESCC KYSE450 cells in the presence of antibodies. The results indicated that 24F-Hu-mut2 had a more pronounced impact on ADCC compared to MGA271 and 24F-Hu-WT group

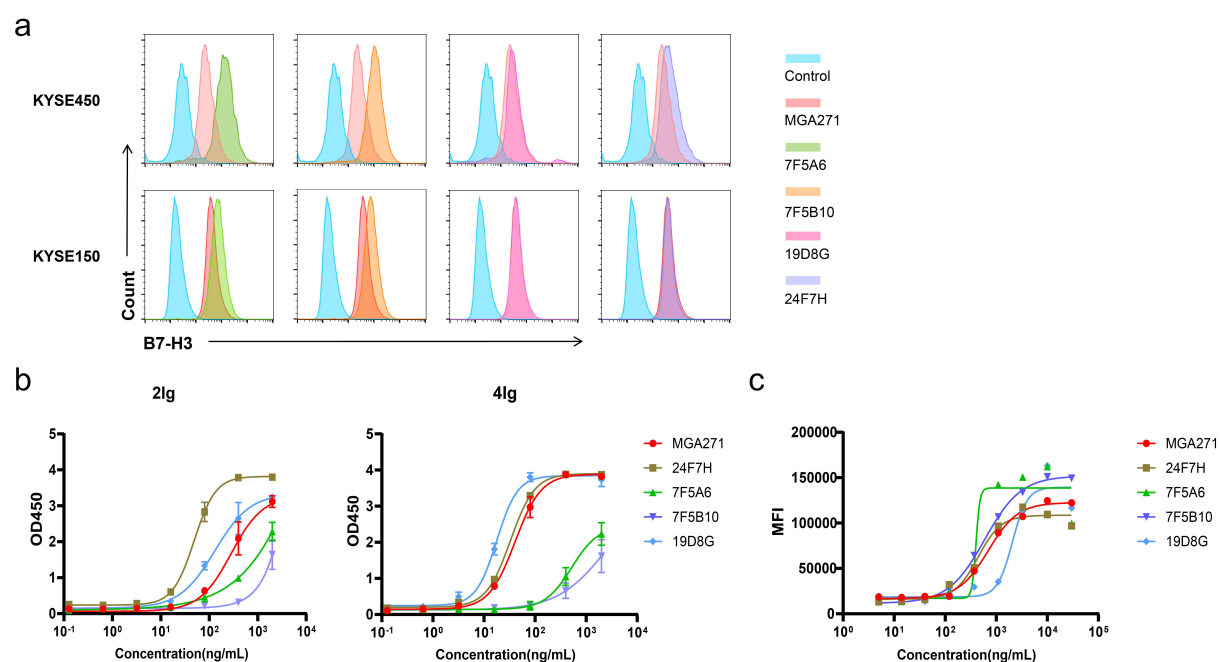


**Figure 2.** Screening of subclones and identification of affinity and bioactivity of murine mAbs. (a) Flow cytometry results showed that all of the four murine antibodies bound to ESCC cell lines. (b) The binding curves of the four murine antibodies to human B7H3-4Ig and B7H3-2Ig as measured by ELISA. (c) The binding curves of four murine antibodies to ESCC cell lines KYSE150 by Flow cytometry.

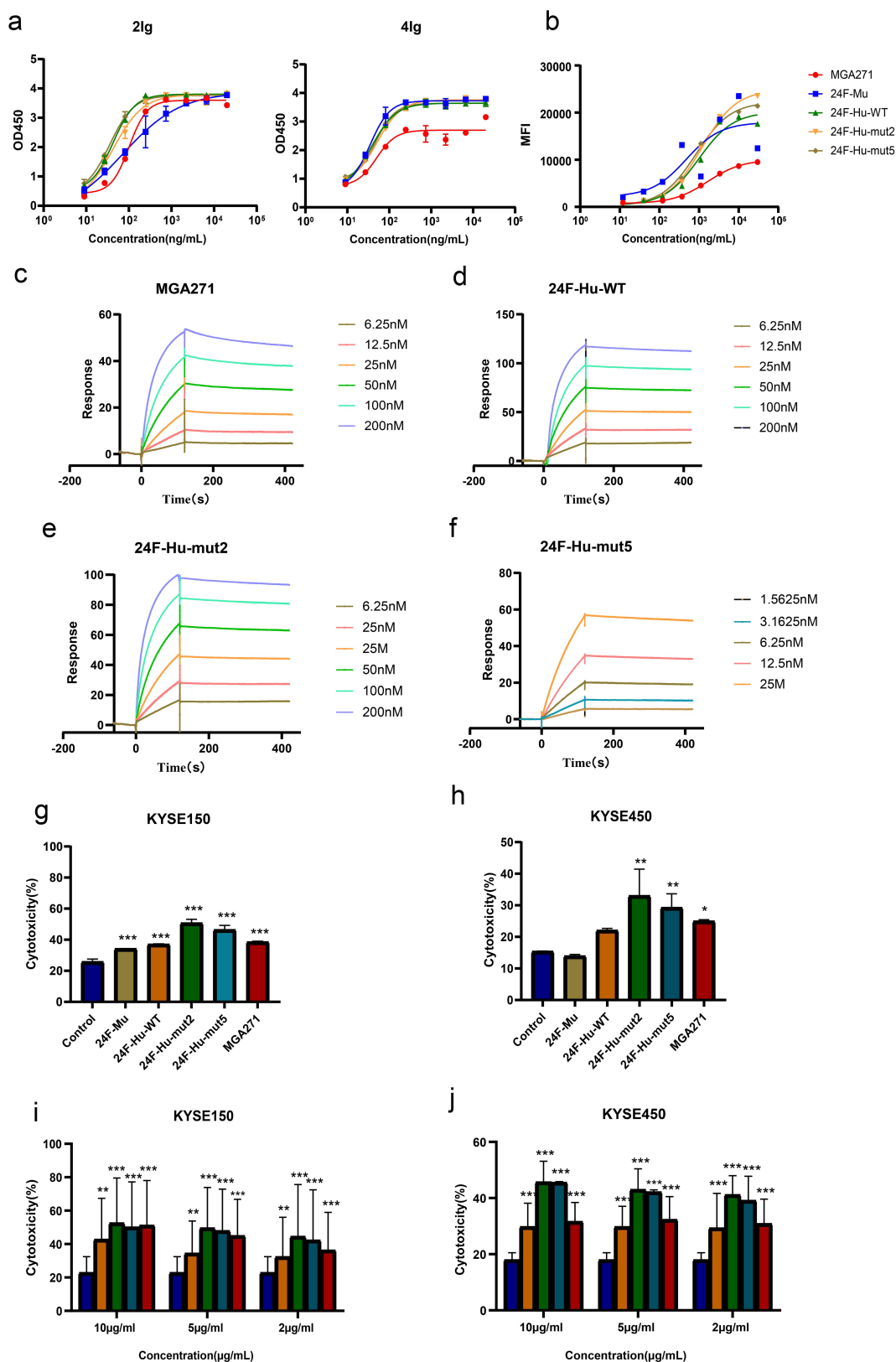


**Figure 3.** The Fc-engineered antibody 24F-Hu-mut2 has high affinity and ADCC activity in vitro. (a) The binding of mAbs to human B7-H3-2Ig and B7-H3-4Ig was analyzed by ELISA. (b) The binding of mAbs to KYSE150 cells was analyzed by Flow cytometry. (c-f) Binding sensorgrams of the captured B7-H3-4Ig interacted with different 24F-Hu-WT Fc mutants. (g-h) LDH assay was used to determine the ability of mAbs to kill KYSE150 and KYSE450 cells by human PBMC in vitro. Effector to target cell ratio (ET ratio) was set to 20:1. (i-j) LDH assay was used to detect the ADCC activity of the monoclonal antibodies against KYSE150 and KYSE450 cells at different concentrations. All data are shown as means  $\pm$  S.D. The asterisks (\*, \*\*, \*\*\*) indicate statistical significance ( $p < .05$ ,  $p < .01$ ,  $p < .001$ , respectively).

**Table 1.** Dissociation constants of MGA271, 24F-Hu-WT, 24F-Hu-mut2 and 24F-Hu-mut5 bound to B7-H3-4Ig.

mAb	ka(1/Ms)	kd(1/s)	KD(nM)
MGA271	$1.38 \times 10^5$	$1.976 \times 10^{-4}$	1.43
24F-Hu-WT	$2.33 \times 10^5$	$1.86 \times 10^{-4}$	0.80
24F-Hu-mut2	$2.11 \times 10^5$	$1.128 \times 10^{-4}$	0.53
24F-Hu-mut5	$3.31 \times 10^5$	$1.65 \times 10^{-4}$	0.50

(Supplement Figure S2C). 24F-Hu-mut2 is therefore a promising antibody based on its affinity for B7-H3 and its cytotoxicity against ESCC cells *in vitro*.

### 24F- Mu and 24F-Hu-WT mAbs binds to the IgC1 and IgC2 domains of B7-H3

B7-H3 (CD276) is a member of the B7 immunomodulator family and involves two isoforms, 4IgB7-H3 (4Ig) and 2IgB7-H3 (2Ig), in humans. The two isoforms have similar structures, with 2Ig in the extracellular immunoglobulin domain IgV-IgC and 4Ig in IgV-IgC-IgV-IgC (Figure 4a), the major subtype expressed in malignant cells.<sup>22,23</sup> B7-H3 exon duplication creates a conserved region in the first IgC domain of 4Ig. This may render 4Ig unable to release the soluble form, whereas 2Ig produces both membrane and soluble forms. B7-H3 has both co-stimulatory and co-inhibitory immunomodulatory functions. It has been reported that 2Ig can increase the proliferation of T cells and the production of IL-2 and IFN- $\gamma$ , while 4Ig can reduce the production of cytokines and the proliferation of T cells.<sup>24</sup> Overexpression of the abnormal B7-H3 protein has been implicated and is associated with poor prognosis in many patients with solid tumors.<sup>25,26</sup> Studies have shown that antibody binding to epitopes closer to the cell membrane is more conducive to the activation of ADCC effect. To verify whether the antibody binds to IgC1 and IgC2, which are closer to the cell membrane, we expressed IgC1 and IgC2 peptides and verified the binding site of parent antibody 24F-Mu by ELISA. The results

showed that 24F-Mu bound to the IgC1 and IgC2 domains of B7-H3 protein (Figure 4b). In order to further elucidated the interaction between B7-H3 antigen and the humanized 24F-Hu-WT antibody, molecular docking simulations were performed. As shown in Figure 4c, it was the IgC domains of B7-H3 antigen that engaged interaction with the 24F-Hu-WT antibody. The VL domain mainly interacted with the IgC2 domain, while the VH domain interacted with both IgC1 and C2 domains. Extensive electrostatic interactions and hydrogen bonding interactions were formed. Specifically, the R223 of IgC1 formed electrostatic interactions with E82 of the VH domain. The sidechains of D230 and Q182 formed hydrogen bonds with S17 and K65, respectively. The main chains of G183 and P185 were hydrogen-bonded with Y60 and R72 of VH domain. For IgC2 domain, E393 formed electrostatic interaction with K52 of VL domain. T409 and T410 were also hydrogen bonded with G56, V57, and A54. In addition, E391 and Y389 also formed hydrogen bond interactions with G101 and K99 of the VH domain. All these interactions contribute to the stabilization of the complex. Based on these results, we concluded that 24F-Hu-WT CDR region binds to the IgC1 and IgC2 domains of human B7-H3.

### 24F-Hu-mut2 inhibits ESCC cell-derived xenograft (CDX) growth

To evaluate the antitumor activity of 24F-Hu-mut2 for ESCC, we conducted a subcutaneous xenograft model using severe combined immunodeficient (SCID) mice (which have

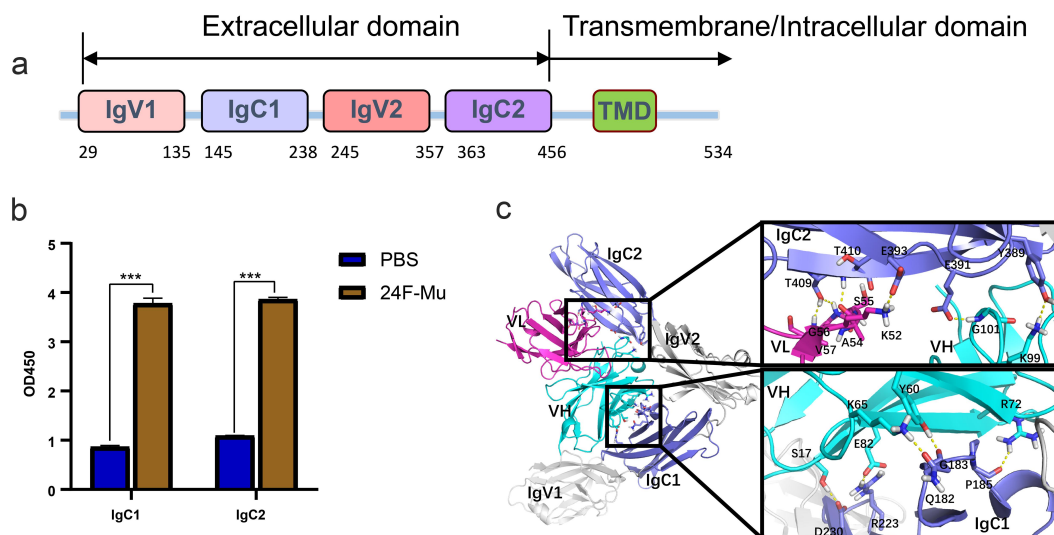


**Figure 4.** 24F- Mu and 24F-Hu-WT mAbs bind to IgC1 and IgC2 domains of B7-H3 protein. (a) Diagram of the protein structure of B7-H3-4Ig. (b) The binding of 24F- Mu to IgC1 and IgC2 domains of B7-H3 protein was detected by ELISA. (c) Molecular docking simulation diagram for mAb 24F-Hu-WT recognition of B7-H3 targets. B7-H3 is shown in the cartoon (IgV1 and IgV2 are shown in gray, while IgC1 and IgC2 are shown in purple). The VH and VL of humanized 24F-Hu-WT are shown in magenta and cyan, respectively. The key interaction residues are shown in sticks. All data are shown as means $\pm$ S.D. The asterisks (\*, \*\*, \*\*\*) indicate statistical significance ( $p < .05$ ,  $p < .01$ ,  $p < .001$ , respectively).

functional NK cells and macrophages). KYSE150 cells ( $2.5 \times 10^6$  per mouse) in PBS were implanted subcutaneously. MGA271, 24F-Hu-mut2, human IgG1 isotype control (5 mg/kg), or vehicle (PBS) were injected intraperitoneally (i.p.) once a week until the average tumor volume of the control group reached about  $1000 \text{ mm}^3$ . The results showed that the tumor volume and weight of the three mAbs groups (MGA271, 24F-Hu-WT and 24F-Hu-mut2) were smaller than those of the control group (Figure 5a-c). These data indicated that the three mAbs inhibited xenograft growth *in vivo*. It is notable that the Fc-engineered 24F-Hu-mut2 mAbs showed a more obvious inhibition of tumor compared with the parental mAbs (24F-Hu-WT) and positive control (MGA271). The body weight of mice did not change significantly during administration (Figure 5d).

### 24F-Hu-mut2 inhibits ESCC patient-derived xenograft (PDX) growth

To further investigate the anti-tumor effect of 24F-Hu-mut2 *in vivo*, we utilized the ESCC PDX model. The mice of case EG20 were treated with MGA271, 24F-Hu-mut2, human IgG1 isotype control (5 mg/kg), or vehicle (PBS) were injected intraperitoneally (i.p.) once a week until the average tumor volume of the control group reached about  $1000 \text{ mm}^3$ . The results showed that the tumor volume and weight of MGA271, 24F-Hu-mut2 and 24F-Hu-mut5 groups were significantly reduced compared with vehicle and human IgG1 groups, demonstrating superior antitumor effect *in vivo*. In addition, the antitumor effect of 24F-Hu-mut2 was better than that of the positive

controls MGA271 and 24F-Hu-mut2 (Figure 6a-c). The weight of the mice in all of the groups did not change significantly during dosing (Figure 6d). To determine NK cell infiltration in PDX model, CD335 and NK1.1 was detected using immunohistochemical staining, which are the molecular markers of mouse NK cells. The results showed that the expression of CD335 and NK1.1 were stronger in the 24F-Hu-mut2 group, indicating that 24F-Hu-mut2 group had more NK cell infiltration in the tumors (Supplement Figure S3).

## Discussion

Here, we developed and thoroughly characterized an Fc-optimized mAb targeting human B7-H3. Studies have shown that B7-H3 is overexpressed in a variety of cancers such as prostate cancer,<sup>27</sup> pancreatic cancer,<sup>26</sup> colorectal cancer,<sup>28</sup> ovarian cancer<sup>29</sup> and bladder cancer,<sup>30</sup> but limited expression in normal tissues and is associated with poor prognosis.<sup>3</sup> We also confirmed the high expression of B7-H3 in an ESCC tissue array by immunohistochemical. In recent years, a variety of B7-H3-targeted immunotherapy strategies, including mAbs, ADC, CAR-T, have been developed and entered preclinical or clinical studies. The monoclonal antibody drug 131I-Omburtamab, for instance, is highly effective in the treatment of CNS/leptomeningeal metastatic neuroblastoma with significant improvement in survival compared to historical data.<sup>31</sup> B7-H3-targeted ADC drug MGC018 has shown promising efficacy in patients with metastatic castration-resistant prostate cancer, and prostate-specific antigen decreased by more than 50% in

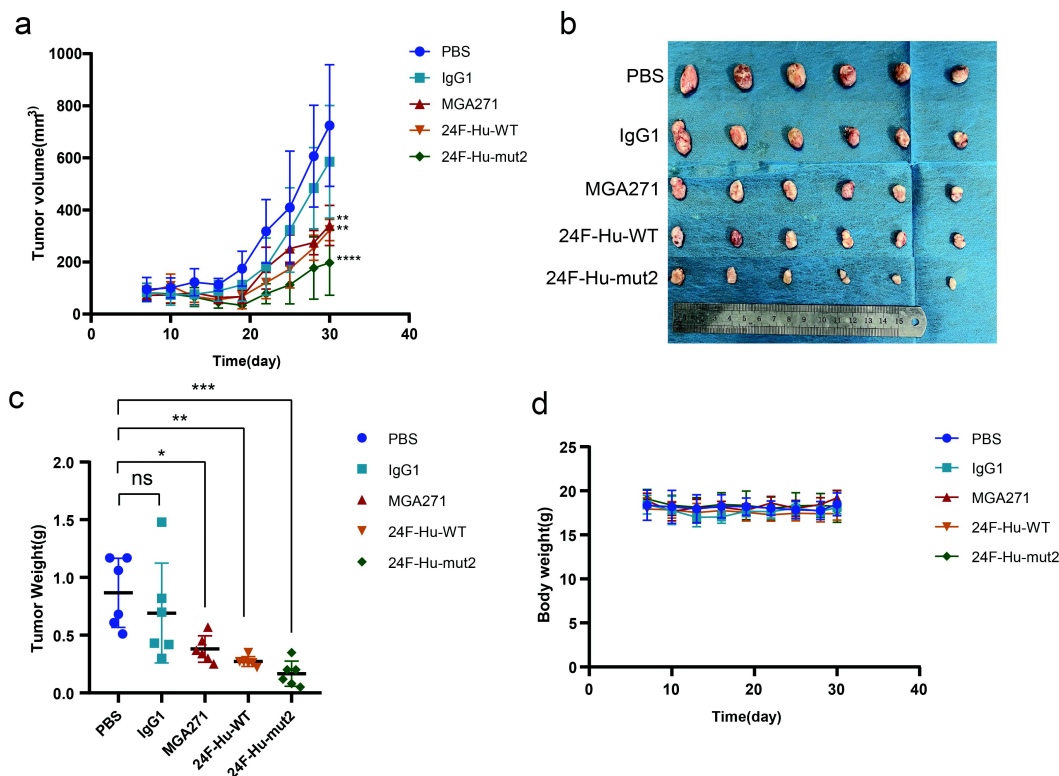


**Figure 5.** 24F-Hu-mut2 inhibits cell derived xenograft (CDX) tumor growth *in vivo*. (a) Tumors growth curves of CDX mice were plotted. 24F-Hu-WT, 24F-Hu-mut2 and MGA271 antibodies and IgG1(5mg/kg) were administrated intraperitoneally once weekly ( $n=6$ ). Tumor volume was measured every 3–4days. (b). Photographs of tumors from each case are shown. (c) Tumor weight after treatment with antibodies ( $n=6$ ). (d) Body weight of mice was measured every 3–4days during treatment with antibody. All data are shown as means $\pm$ S.D. The asterisks (\*, \*\*, \*\*\*) indicate statistical significance ( $p < .05$ ,  $p < .01$ ,  $p < .001$ , respectively).



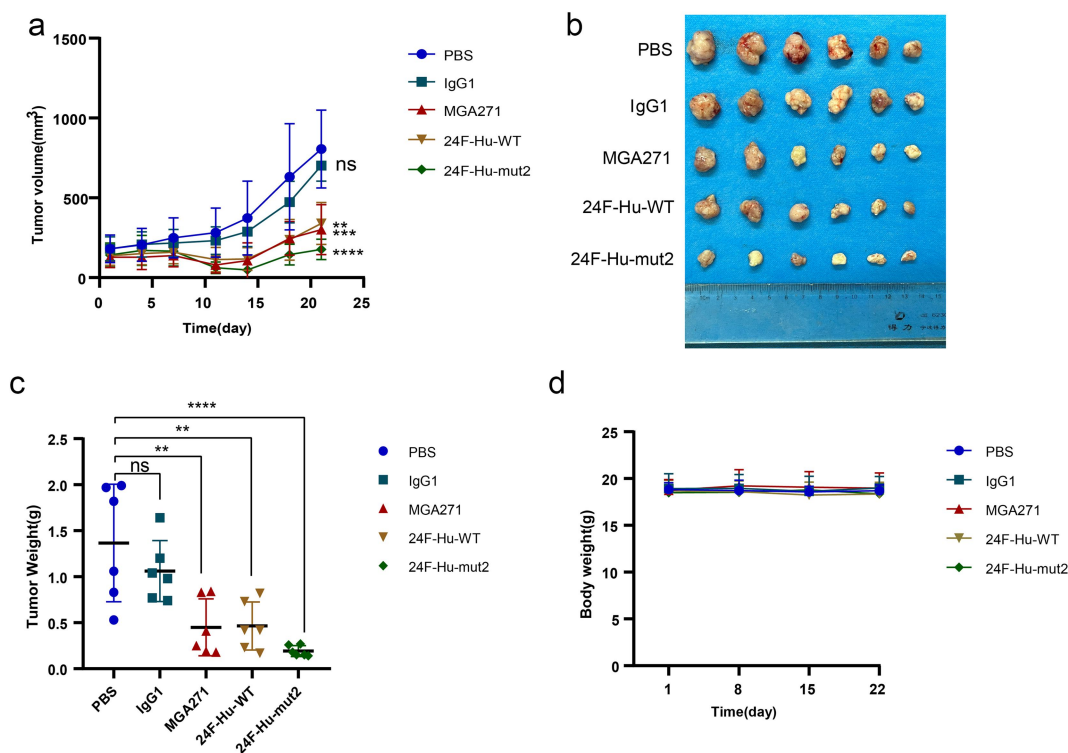


**Figure 6.** 24F-Hu-mut2 inhibits patient-derived xenograft (PDX) tumor growth *in vivo*. (a) Tumors growth curves of PDX mice were plotted. 24F-Hu-WT, 24F-Hu-mut2 and MGA271 antibodies and IgG1(5mg/kg) were administrated intraperitoneally once weekly ( $n=6$ ). Tumor volume was measured every 3–4days. (b) Photographs of tumors from each case are shown. (c) Tumor weight after treatment with antibodies ( $n=6$ ). (d) Body weight of mice was measured weekly during treatment with antibody. All data are shown as means $\pm$ S.D. The asterisks (\*, \*\*, \*\*\*) indicate statistical significance ( $p < .05$ ,  $p < .01$ ,  $p < .001$ , respectively).

50% of patients (NCT03729596). These indicate that B7-H3 is a safe and effective target for anticancer drug development.

MABs are the most commonly used tumor immunotherapy in clinical practice.<sup>32</sup> The therapeutic effects of antibodies are based on the affinity of the Fv region of an antibody to the target at nanomolar levels and the ability of the Fc region of an antibody to engage components of the host immune system.<sup>33</sup> However, according to the current clinical research data of esophageal cancer, the efficacy of therapeutic mAbs is not significant. It is worth mentioning that these clinical data are mostly from esophageal adenocarcinoma or esophagogastric junction cancer and there are few studies on ESCC. Therefore, it is necessary to further explore the suitable mAbs for ESCC. ADCC is a very important mechanism for monoclonal antibodies to play an anti-tumor role, which mainly depends on the recognition of Fc region of antibodies with Fc $\gamma$  receptors of natural killer (NK) cells and other immune cells. Examples of monoclonal antibodies with ADCC properties include Rituximab targeting CD20 and trastuzumab targeting HER2 protein, which have been applied to the clinical treatment of breast cancer and lymphoma and have shown good clinical efficacy.<sup>34,35</sup> Many mutations in the Fc domain of antibody have been found to directly or indirectly enhance the binding capacity to Fc $\gamma$  receptors, thereby significantly enhancing cytotoxicity. Lazar et al. identified S239D/A330L/I332E mutants to enhance cytotoxicity.<sup>13</sup> And targeted B7-H3 MGA271 mAb with L235V/F243L/R292P/Y300L/P396L mutants enhance the affinity for the human activated Fc $\gamma$  receptor CD16A and reduce the affinity for the human inhibited Fc $\gamma$  receptor CD32B.<sup>36</sup> Fc modification of MGA271 significantly enhanced

the anti-tumor effect *in vivo*. In this study, two Fc-optimized antibodies were developed after hybridoma screening and humanization. 24F-Hu-mut5 modified the Fc fragment at the same site as the positive antibody MGA271. The ADCC activity of 24F-Hu-mut5 was significantly increased compared with that of 24F-Hu-WT. The other is to convert the humanized 24F-Hu-WT into 24F-Hu-mut2 based on XmAb5574 (containing S239D/I332E mutation). XmAb5574 has a high affinity for human Fc $\gamma$ RIIIa and Fc $\gamma$ RIIa, which in turn improved the ability of the antibody to mediate ADCC.<sup>37</sup> Our results showed that the Fc-optimized antibody 24F-Hu-mut2 showed greater antitumor activity compared to 24F-Hu-WT and 24F-Hu-mut5. Therefore, we selected 24F-Hu-mut2 for animal experiments. As expected, 24F-Hu-mut2 exhibited superior antitumor effects in both ESCC CDX and PDX models without obvious toxic effects. This also demonstrates that 24F-Hu-mut2 has great potential as a therapeutic antibody.

We know that B7-H3 exists in both B7-H3-4Ig and B7-H3-2Ig forms, with humans predominating on B7-H3-4Ig.<sup>38</sup> B7-H3-4Ig protein extracellular region consists of four domains: IgV1, IgC1, IgV2, and IgC2. When the recognition region of an antibody binds to the antigen located in tumor cell membrane, its Fc segment binds to the FcR of NK cell, macrophages and other immune cells to kill tumor cells.<sup>39</sup> During the initial screening, we confirmed that Murine parental antibody 24F-Mu could bind to the IgC1 and IgC2 domains of B7-H3 by ELISA. Moreover, the results of the computer docking model showed the VH and VL of 24F-Hu-WT interact with both IgC1 and IgC2

domains. In terms of the spatial structure of B7-H3 molecule, IgC1 and IgC2 were closer to the cell membrane than IgV1 and IgV2. Studies had shown that ADCC had a preference for membrane proximal epitopes.<sup>40</sup> Therefore, 24F-Hu-WT mAb can recognize IgC1 and IgC2, which can promote more efficient killing of tumor cells by immune cells.

The expression of B7-H3 on tumor-associated vascular endothelial cells suggests that B7-H3 has an additional role in promoting tumor growth and progression.<sup>41</sup> However, mAbs targeting B7-H3 may cause vascular endothelial damage and increase the risk of bleeding. Further studies are needed to avoid these potential risks. In addition, the B7-H3 receptor is not yet identified, preserving the possibility for 24F-Hu-mut2 to play other roles, such as directly reversing immunosuppression and promoting tumor cell clearance. These uncharted areas remain to be explored.

In summary, we developed a B7-H3-targeting mAb 24F-Hu-mut2, which is Fc-engineered with significant antitumor activity in ESCC *in vitro* and *in vivo*. And it has potential as a novel therapeutic monoclonal antibody for the treatment of esophageal cancer and other B7-H3 over-expressing tumors.

## Disclosure statement

No potential conflict of interest was reported by the author(s).

## Funding

This study was supported by the National Natural Science Foundation of China (Grant no. 81872335), the Science Foundation of Henan Education Department (Grant no. 23A310018), the Central Plains Science and Technology Innovation Leading Talents (No.224200510015) and the Supporting Plan of Scientific and Technological Innovation Team in Universities of Henan Province (No. 20IRTSTHN029).

## Authors contributions

J.Z., K.L. designed experiments and revised the paper. H.W., C.L. and Q.Y. performed experiments and wrote the paper. Y.Q. performed the computational docking model. Y.D., L.D., W.L., M.Z. and X. Z. contributed reagents or other essential material. J.L., Y.J. and J. L. assisted with analyzed data. Z.D. supervised designed experiments. All authors contributed to the article and approved the submitted version.

## Ethics approval

After density gradient centrifugation over Ficoll, PBMC were acquired from blood samples of healthy donors in compliance with protocols approved by Zhengzhou University Review Board. All protocols of mouse study were approved by Zhengzhou University Review Board.

## References

- Abnet CC, Arnold M, Wei WQ. Epidemiology of esophageal squamous cell carcinoma. *Gastroenterology*. 2018;154(2):360–373. doi:10.1053/j.gastro.2017.08.023.
- Hsieh CH, Kuan WH, Chang WL, Kuo I-Y, Liu H, Shieh D-B, Liu H, Tan B, Wang Y-C. Dysregulation of SOX17/NRF2 axis confers chemoradiotherapy resistance and emerges as a novel therapeutic target in esophageal squamous cell carcinoma. *J Biomed Sci*. 2022;29:90. doi:10.1186/s12929-022-00873-4.
- Dong P, Xiong Y, Yue J, Hanley S, Watari H. B7H3 as a promoter of metastasis and promising therapeutic target. *Front Oncol*. 2018;8:264. doi:10.3389/fonc.2018.00264.
- Wang J, Chong KK, Nakamura Y, Nguyen L, Huang SK, Kuo C, Zhang W, Yu H, Morton DL, Hoon DSB, et al. B7-H3 associated with tumor progression and epigenetic regulatory activity in cutaneous melanoma. *J Invest Dermatol*. 2013;133(8):2050–2058. doi:10.1038/jid.2013.114.
- Kontos F, Michelakos T, Kurokawa T, Sadagopan A, Schwab JH, Ferrone CR, Ferrone S. B7-H3: an attractive target for antibody-based immunotherapy. *Clin Cancer Res*. 2021;27:1227–1235. doi:10.1158/1078-0432.CCR-20-2584.
- Zhou WT, Jin WL. B7-H3/CD276: An Emerging Cancer Immunotherapy. *Front Immunol*. 2021;12:701006. doi:10.3389/fimmu.2021.701006.
- Janakiram M, Shah UA, Liu W, Zhao A, Schoenberg MP, Zang X. The third group of the B7-CD28 immune checkpoint family: HHLA2, TMIGD2, B7x, and B7-H3. *Immunol Rev*. 2017;276(1):26–39. doi:10.1111/imr.12521.
- Leitner J, Klausner C, Pickl WF, Stöckl J, Majdic O, Bardet AF, Kreil DP, Dong C, Yamazaki T, Zlabinger G, et al. B7-H3 is a potent inhibitor of human T-cell activation: no evidence for B7-H3 and TREML2 interaction. *Eur J Immunol*. 2009;39(7):1754–1764. doi:10.1002/eji.200839028.
- Picarda E, Ohaegbulam KC, Zang X. Molecular pathways: targeting B7-H3 (CD276) for human cancer immunotherapy. *Clin Cancer Res*. 2016;22(14):3425–3431. doi:10.1158/1078-0432.CCR-15-2428.
- Chen L, Chen J, Xu B, Wang, Qi, Zhou W, Zhang G, Sun J, Shi L, Pei H, Wu C, Jiang J, et al. B7-H3 expression associates with tumor invasion and patient's poor survival in human esophageal cancer. *Am J Transl Res*. 2015;7:2646–60.
- Ahmed M, Cheng M, Zhao Q, Goldgur Y, Cheal SM, Guo H-F, Larson SM, Cheung NKV. Humanized affinity-matured monoclonal antibody 8H9 has potent antitumor activity and binds to FG loop of tumor antigen B7-H3. *J Biol Chem*. 2015;290:30018–30029. doi:10.1074/jbc.M115.679852.
- Stavenhagen JB, Gorlatov S, Tuaille N, Rankin CT, Li H, Burke S, Huang L, Johnson S, Bonvini E, Koenig S, et al. Fc Optimization of therapeutic antibodies enhances their ability to kill tumor cells *in vitro* and controls tumor expansion *in vivo* via low-affinity activating Fcγ receptors. *Cancer Res*. 2007;67:8882–8890. doi:10.1158/0008-5472.CAN-07-0696.
- Lazar GA, Dang W, Karki S, Vafa O, Peng JS, Hyun L, Chan C, Chung HS, Eivazi A, Yoder SC, et al. Engineered antibody Fc variants with enhanced effector function. *Proc Natl Acad Sci USA*. 2006;103(11):4005–4010. doi:10.1073/pnas.0508123103.
- Jumper J, Evans R, Pritzel A, Green T, Figurnov M, Ronneberger O, Tunyasuvunakool K, Bates R, Židek A, Potapenko A, et al. Highly accurate protein structure prediction with AlphaFold. *Nature*. 2021;596(7873):583–589. doi:10.1038/s41586-021-03819-2.
- Varadi M, Anyango S, Deshpande M, Nair S, Natassia C, Yordanova G, Yuan D, Stroe O, Wood G, Laydon A, et al. AlphaFold protein structure database: massively expanding the structural coverage of protein-sequence space with high-accuracy models. *Nucleic Acids Res*. 2022;50(D1):D439–D444. doi:10.1093/nar/gkab1061.
- Sivasubramanian A, Sircar A, Chaudhury S, Gray JJ. Toward high-resolution homology modeling of antibody fv regions and application to antibody-antigen docking. *Proteins*. 2009;74:497–514. doi:10.1002/prot.22309.
- Marze NA, Lyskov S, Gray JJ. Improved prediction of antibody VL-VH orientation. *Protein Eng Des Sel*. 2016;29:409–418. doi:10.1093/protein/gzw013.
- Weitzner BD, Gray JJ. Accurate structure prediction of CDR H3 loops enabled by a novel structure-based C-Terminal constraint. *J Immunol*. 2017;198(1):505–515. doi:10.4049/jimmunol.1601137.

19. Weitzner BD, Jeliakov JR, Lyskov S, Marze N, Kuroda D, Frick R, Adolf-Bryfogle J, Biswas N, Dunbrack RL, Gray JJ, et al. Modeling and docking of antibody structures with Rosetta. *Nat Protoc.* 2017;12(2):401–416. doi:10.1038/nprot.2016.180.
20. Lyskov S, Chou FC, Conchuir SO, Der BS, Drew K, Kuroda D, Xu J, Weitzner BD, Renfrew PD, Sripakdeevong P, et al. Serverification of molecular modeling applications: the Rosetta online server that includes everyone (ROSIE). *PloS One.* 2013;8:e63906. doi:10.1371/journal.pone.0063906.
21. Pierce BG, Hourai Y, Weng Z, Keskin O. Accelerating protein docking in ZDOCK using an advanced 3D convolution library. *PloS One.* 2011;6(9):e24657. doi:10.1371/journal.pone.0024657.
22. Steinberger P, Majdic O, Derdak SV, Pfistershammer K, Kirchberger S, Klauser C, Zlabinger G, Pickl WF, Stöckl J, Knapp W, et al. Molecular characterization of human 4Ig-B7-H3, a member of the B7 family with four ig-like domains. *J Immunol.* 2004;172(4):2352–2359. doi:10.4049/jimmunol.172.4.2352.
23. Zhou YH, Chen YJ, Ma ZY, Xu L, Wang Q, Zhang G-B, Xie F, Ge Y, Wang X-F, Zhang X-G, et al. 4IgB7-H3 is the major isoform expressed on immunocytes as well as malignant cells. *Tissue Antigens.* 2007;70(2):96–104. doi:10.1111/j.1399-0039.2007.00853.x.
24. Sun J, Fu F, Gu W, Yan R, Zhang G, Shen Z, Zhou Y, Wang H, Shen B, Zhang X, et al. Origination of new immunological functions in the costimulatory molecule B7-H3: the role of exon duplication in evolution of the immune system. *PloS One.* 2011;6(9):e24751. doi:10.1371/journal.pone.0024751.
25. Yuan H, Wei X, Zhang G, Li C, Zhang X, Hou J. B7-H3 over expression in prostate cancer promotes tumor cell progression. *J Urol.* 2011;186(3):1093–1099. doi:10.1016/j.juro.2011.04.103.
26. Zhao X, Li DC, Zhu XG, GAN W-J, LI Z, XIONG F, ZHANG Z-X, ZHANG G-B, ZHANG X-G, ZHAO H, et al. B7-H3 overexpression in pancreatic cancer promotes tumor progression. *Int J Mol Med.* 2013;31(2):283–291. doi:10.3892/ijmm.2012.1212.
27. Zang X, Thompson RH, Al-Ahmadie HA, Serio AM, Reuter VE, Eastham JA, Scardino PT, Sharma P, Allison JP. B7-H3 and B7x are highly expressed in human prostate cancer and associated with disease spread and poor outcome. *Proc Natl Acad Sci USA.* 2007;104:19458–19463. doi:10.1073/pnas.0709802104.
28. Ingebrigtsen VA, Boye K, Tekle C, Nesland JM, Flatmark K, Fodstad O. B7-H3 expression in colorectal cancer: nuclear localization strongly predicts poor outcome in colon cancer. *Int J Cancer.* 2012;131:2528–2536. doi:10.1002/ijc.27566.
29. Zang X, Sullivan PS, Soslow RA, Waitz R, Reuter VE, Wilton A, Thaler HT, Arul M, Slovin SF, Wei J, et al. Tumor associated endothelial expression of B7-H3 predicts survival in ovarian carcinomas. *Mod Pathol.* 2010;23(8):1104–1112. doi:10.1038/modpathol.2010.95.
30. Xylinas E, Robinson BD, Kluth LA, Volkmer BG, Hautmann R, Küfer R, Zerbib M, Kwon E, Thompson RH, Boorjian SA, et al. Association of T-cell co-regulatory protein expression with clinical outcomes following radical cystectomy for urothelial carcinoma of the bladder. *Eur J Surg Oncol.* 2014;40(1):121–127. doi:10.1016/j.ejso.2013.08.023.
31. Kramer K, Pandit-Taskar N, Kushner BH, Zanzonico P, Humm JL, Tomlinson U, Donzelli M, Wolden SL, Haque S, Dunkel I, et al. Phase 1 study of intraventricular (131)I-omburtamab targeting B7H3 (CD276)-expressing CNS malignancies. *J Hematol Oncol.* 2022;15:165. doi:10.1186/s13045-022-01383-4.
32. Kimiz-Gebologlu I, Gulce-Iz S, Biray-Avci C. Monoclonal antibodies in cancer immunotherapy. *Mol Biol Rep.* 2018;45(6):2935–2940. doi:10.1007/s11033-018-4427-x.
33. Harris TJ, Drake CG. Primer on tumor immunology and cancer immunotherapy. *J Immunother Cancer.* 2013;1:12. doi:10.1186/2051-1426-1-12.
34. Mossner E, Brunker P, Moser S, Püntener U, Schmidt C, Herter S, Grau R, Gerdes C, Nopora A, van Puijenbroek E, et al. Increasing the efficacy of CD20 antibody therapy through the engineering of a new type II anti-CD20 antibody with enhanced direct and immune effector cell-mediated B-cell cytotoxicity. *Blood.* 2010;115:4393–4402. doi:10.1182/blood-2009-06-225979.
35. Schlam I, Nunes R, Lynce F. Profile of Margetuximab: evidence to date in the targeted treatment of metastatic HER2-positive breast cancer. *Onco Targets Ther.* 2022;15:471–478. doi:10.2147/OTT.S272197.
36. Loo D, Alderson RF, Chen FZ, Huang L, Zhang W, Gorlatov S, Burke S, Ciccarone V, Li H, Yang Y, et al. Development of an Fc-enhanced anti-B7-H3 monoclonal antibody with potent antitumor activity. *Clin Cancer Res.* 2012;18:3834–3845. doi:10.1158/1078-0432.CCR-12-0715.
37. Awan FT, Lapalombella R, Trotta R, Butchar JP, Yu B, Benson DM, Roda JM, Cheney C, Mo X, Lehman A, et al. CD19 targeting of chronic lymphocytic leukemia with a novel Fc-domain-engineered monoclonal antibody. *Blood.* 2010;115:1204–1213. doi:10.1182/blood-2009-06-229039.
38. Zhang W, Zhang L, Qian J, Lin J, Chen Q, Yuan Q, Zhou J, Zhang T, Shi J, Zhou H, et al. Expression characteristic of 4Ig B7-H3 and 2Ig B7-H3 in acute myeloid leukemia. *Bioengineered.* 2021;12(2):11987–12002. doi:10.1080/21655979.2021.2001182.
39. Nagase-Zembutsu A, Hirotani K, Yamato M, Yamaguchi J, Takata I, Yoshida M, Fukuchi K, Yazawa M, Takahashi S, Agatsuma T, et al. Development of DS-5573a: a novel afucosylated mAb directed at B7-H3 with potent antitumor activity. *Cancer Sci.* 2016;107(5):674–681. doi:10.1111/cas.12915.
40. Cleary K, Chan H, James S, Glennie MJ, Cragg MS. Antibody distance from the cell membrane regulates antibody effector mechanisms. *J Immunol.* 2017;198(10):3999–4011. doi:10.4049/jimmunol.1601473.
41. Seaman S, Zhu Z, Saha S, Zhang XM, Yang MY, Hilton MB, Morris K, Szot C, Morris H, Swing DA, et al. Eradication of tumors through simultaneous ablation of CD276/B7-H3-positive tumor cells and tumor vasculature. *Cancer Cell.* 2017;31:501–515. doi:10.1016/j.ccell.2017.03.005.